Efficient Anomalous Forcings for Linear Problems

Li Zhijin (李志锦) and *Ji Liren* (纪立人)
Institute of Atmospheric Physics, Chinese Academy of Sciences, Beijing 100080
Received November 1, 1993; revised June 10, 1994

ABSTRACT

For linear forcing problems, a method is developed to provide a set of forcing modes which form a complete orthonormal basis for the finite-time response to steady forcing in the energy inner product space. The forcing modes are found by calculating eigenvectors of a positive definite and symmetric matrix determined from given equations of motion. The amplitude of responses to forcing modes is given in terms of the associated eigenvalues. This method is used in a nondivergent barotropic model linearized about the 300 hPa zonally-varying climatological flow both for northern summertime and wintertime. The results show that the amplitude of response varies considerably with different forcing modes. Only a few of forcing modes associated with the leading eigenvalues, called efficient forcing mode, can excite significant response. The efficient forcing modes possess highly localized spatial structure with wavetrain appearance. Most of the efficient forcings are located to the south of regions of the jet cores. The forcings located over polar regions are also efficient. In addition, the response is larger in wintertime than in summertime for a given forcing.

Key words: Generalized eigenvalue and eigenvector; Strength factor of response; Efficient forcing

I. INTRODUCTION

The general circulations have apparent features of the latitudinal and longitudinal variation and seasonal cycles. Naturally, the role of anomalous external sources in the atmospheric variations is greatly influenced by these features. In order to understand the dynamical processes of the generation of atmospheric anomalies by forcing anomalies, it is necessary to determine these influences of the features of the general circulation.

Some previous studies have shown that the amplitude of a response to a forcing depends on the geographical position of the forcing. For example, Keshavamurty (1982) has investigated the sensitivity of the general circulation model (GCM) to the warm sea surface temperature anomaly (SSTA) located at various regions over the equatorial Pacific, and found that the SSTA at middle equatorial Pacific can excite flow anomalies more easily than that at eastern equatorial Pacific. The numerical studies by Simmons (1982) have indicated that the forcing located to the south of the regions of strong flow can produce a large response. The detailed studies by Simmons et al. (1983) and Branstator (1985) with simple and idealized model further identified the results from GCM experiments. Chinese researchers (Huang et al. (1988) and Fu et al. (1988)) have also long understood that the intensification of heat sources associated with the convective activities over the South China Sea, Philippine and west equatorial Pacific can significantly influence the generation of atmospheric flow anomalies over the Northern Hemisphere, and it is also shown that the influence of the SSTA over east equatorial Pacific is not obvious. These studies have suggested that only the forcings located in the efficient regions, which are determined by the local structure of the background flow, can excite

large responses. This result can not be explained by the theory of the Rossby wave ray certainly (see Hoskins. et al., 1981). However, what are the features of the efficient forcing which excite large response? It is insufficient to provide complete answer only by the numerical experiments like previous studies. New approaches should be found, which is just the purpose of this study.

II. MODEL DESCRIPTION

Considering the nondivergent barotropic vorticity equation with a forcing and dissipation

$$\frac{\partial \zeta}{\partial t} + J(\psi,\ \zeta + f) + K\nabla^4\ \zeta + \gamma\zeta = F\ , \tag{1}$$

where $\zeta = \nabla^2\psi$, F is a prescribed external source, others are the same as commonly used. Eq.(1) is often used in the studies on forcing problems (see Lau et al., 1992 and Hoskins et al., 1993).

The quantities of the climatological state are barred, and the governing equation for them may be written as

$$J(\bar{\psi},\ \bar{\zeta} + f) + K\nabla^4\ \bar{\zeta} + \gamma\bar{\zeta} = \bar{F}\ , \tag{2}$$

where $\bar{F}$ stands for the forcing which is required to sustain the zonally-varying climatological flow. Therefore, we can have the equations linearized about the climatological flow:

$$\frac{\partial \zeta'}{\partial t} + J(\bar{\psi},\ \zeta') + J(\psi', \bar{\zeta} + f) + K\nabla^4\ \zeta' + \gamma\zeta' = F'\ , \tag{3}$$

where the quantities of anomalous perturbation are primed.

Equation (3) is solved in spherical coordinates by using a spectral technique. The variables are expressed in terms of spherical harmonics. The equations are triangularly truncated at 21. So we have

$$\bar{\zeta} = \sum_{m=-J}^{J} \sum_{n=|m|}^{J} \bar{\zeta}_{mn} P_n^m(\mu) e^{im\lambda}\ , \tag{4}$$

$$\zeta' = \sum_{m=-J}^{J} \sum_{n=|m|}^{J} \zeta_{mn} P_n^m(\mu) e^{im\lambda}\ , \tag{5}$$

where $J = 21$, φ is the latitude, λ the longitude, $\mu = \sin\varphi$, and P_n^m is the associated Legendrian function. From (4) and (5), we have

$$\bar{\psi} = -\sum_{m=-J}^{J} \sum_{n=|m|}^{J} \bar{\zeta}_{mn} P_n^m(\mu) e^{im\lambda} / C_n^2\ , \tag{6}$$

$$\psi = -\sum_{m=-J}^{J} \sum_{n=|m|}^{J} \bar{\zeta}_{mn} P_n^m(\mu) e^{im\lambda} / C_n^2\ , \tag{7}$$

where $C_n^2 = n(n+1)$. F' can also be written as

$$F' = \sum_{m=-J}^{J} \sum_{n=|m|}^{J} F_{mn} P_n^m(\mu) e^{im\lambda}\ . \tag{8}$$

Substituting (4)–(8) into (3), (3) can be represented in the spectral form by using the Galerkian approximation:

$$\frac{dx}{dt} = Ax + f \ , \tag{9}$$

where x and f are vectors that contain the nonzero real and imaginary part of the spectral coefficient of the vorticity field ζ' and the forcing field F' respectively. A is a real matrix. Following the method described by Hoskins et al. (1981), the jth column of A is found by evaluating the spectral versions of the unforced right–hand side of Eq.(3) for a perturbation field that is zero in all but jth coefficient. A is an asymmetric matrix, determined only by the meridional and zonal variations in the basic flow. Considering the angular momentum conservation constraint, ζ_{00}, ζ_{01} and ζ_{11} should be taken as zero. So Eq.(9) is a linear system of equations with the order of $N = (J+1)(J+2) - (J+1) - 4 = 480$, which is used as basic model in this study.

III. EFFICIENT FORCING

In order to define a strength factor of a response to a given external forcing and introduce a complete and orthogonal basis, we have chosen an inner product such that

$$(y, z) = y^T Dz = z^T Dy \ , \tag{10}$$

where y and z are vectors, "T" stands for a matrix transposition. The norm of a vector y is $\|y\| = \sqrt{(y,y)}$. D should be a positive definite and symmetric matrix. In this study, D is a diagonal matrix, and is taken as

$$D_{ij} = 0, \qquad \text{if} \quad i \neq j;$$
$$D_{ij} = 1 / 2C_j^{2(2-s)}, \ \text{if} \quad i = j \quad \text{and} \quad m = 0;$$
$$D_{ij} = 1 / C_j^{2(2-s)}, \ \text{if} \quad i = j \quad \text{and} \quad m \neq 0.$$

Since x is composed of the spectral coefficient of spherical harmonics, we have results: if $s = 0$, $\|x\|^2$ is the global streamfunction square; if $s = 1$, $\|x\|^2$ twice the global kinetic energy; if $s = 2$, $\|x\|^2$ the global enstrophy. They all can be called energy norm.

Supposing $x(0) = 0$, we have the solution to Eq.(9):

$$x = \int_0^t e^{A(t-s)} f ds \ , \tag{11}$$

where $x(t)$ is just the response to a forcing anomaly at time t, and

$$e^{At} = I + \frac{At}{1!} + \frac{A^2 t^2}{2!} + \frac{A^3 t^3}{3!} + \cdots\cdots \tag{12}$$

(12) is convergent for any given t. If A is not singular, it is easily to prove that (12) can be differentiated and integrated by terms with respect to t.

Considering a steady forcing, a strength factor of response can be defined as $\sigma(t)$:

$$\sigma(t) = \|x\| / \|f\| \ . \tag{13}$$

One can see that $\sigma(t)$ is the amplitude of the response at time t to a unit forcing. The larger $\sigma(t)$ is, the more efficiently the forcing excites a response.

Let $B = \int_0^t e^{A(t-s)} ds$. From Eq.(11), the perturbation norm at time t is given by

$$\|x\|^2 = f^T B^T DBf . \tag{14}$$

And let $H = B^T DB$, it is easy to find that H is a positive definite and symmetric matrix. Let a vector v and a number λ satisfy

$$Hv = \lambda Dv , \tag{15}$$

where v is called a generalized eigenvector, and λ a generalized eigenvalue. Since D is a diagonal matrix, it can be decomposed as: $D = DL^T$. Substituting it into (15), we yield

$$(L^{-1} HL^{-T})(L^T v) = \lambda L^T v . \tag{16}$$

Let $G = L^{-1}HL^{-T}$, G is also a positive definite and symmetric matrix. if $u_j (j = 1, 2, 3, \cdots, N)$ are the eigenvectors of the matrix G, they will form a complete orthonormal basis in the Euclidean space.

If $u_j = L^T v_j$, we have

$$v_j = L^{-T} u_j . \tag{17}$$

Then

$$(v_i, v_j) = v_i^T Dv_j = u_i L^{-1} DL^{-T} u_j = u_i u_j = \begin{cases} 0 & i \neq j , \\ 1 & i = j . \end{cases} \tag{18}$$

Thus, it has been shown that $v_j (j = 1, 2, 3, , \cdots, N)$ form a complete orthonormal basis in the given energy inner product space. From here, the eigenvalues are in descent order.

If a forcing f is parallel to an eigenvector v_j, we get from (14)

$$\sigma_i(t) = \lambda_i . \tag{19}$$

Eq.(19) is important and indicates that if a forcing f is parallel to the eigenvector associated with a large eigenvalue, the response is large. Hereafter, an eigenvector is also referred to as a forcing mode.

For any given forcing f, the expansion onto eigenvectors can be expressed as

$$f = \sum_{j=1}^{N} (f, v_j) v_j = \sum_{j=1}^{N} f_j v_j , \tag{20}$$

where f_j is the projection of the forcing f onto the eigenvector v_j. Substituting (20) into (14), we obtain

$$\sigma(t) = \left(\sum_{j=1}^{N} \frac{f_j^2}{\|f\|^2} \lambda_j \right) . \tag{21}$$

From (21), we obtain easily

$$\sum_{j=1}^{N} f_j^2 / \|f\|^2 = 1 . \tag{22}$$

From (21) and (22), we can reach conclusions that the strength factor of a response to a given forcing depends on the magnitude of the generalized eigenvalues and the projections of the forcing onto the forcing modes (the former is the reflection of the influences of the basic state, the latter the reflection of the role of the structure of the forcing). The larger the projections of a forcing on the forcing modes associated with large eigenvalues, the larger response it produces.

The discussion above has shown that in order to find the efficient forcings, it is only required to calculate the generalized eigenvectors and eigenvalues of a positive definite and symmetric matrix from the given equations of motion. Since the eigenvalue determines the strength factor of a response to a forcing mode, the leading eigenvectors are naturally the efficient forcing modes.

IV. RESULT PRESENTATION

The basic state used in this study is the 300 hPa climatological flow in the northern wintertime and summertime respectively, which comes from the 10 years of ECMWF analyses from 1980 to 1989. The streamfunctions are symmetric about the equator. The matrix B is computed as the exponential of A using a Taylor expansion. The analysis of barotropic instability of normal mode shows that the largest unstable growth rate has the e–folding time of 8.3 days for wintertime. The drag coefficient γ is assigned a value of 1 / (7 days), so that the instability of normal mode is removed. The diffusion coefficient K is taken as zero. The kinetic energy norm is employed.

1. *Wintertime*

Table 1 shows the strength factors of response corresponding to the first 20 forcing modes for the evolution time $t = 48$ hours. It can be seen that the strength factors decrease considerably rapidly with the order index. From Table 1, the 10th strength factor decreases by about a factor of 2 compared with the first one, and the 20th about a factor of 3 compared with the first one. These results indicate that only if an anomalous forcing has large projection onto the subspace which is spanned by a few forcing modes associated with the large eigenvalues, it will excite a response efficiently.

Table 1. Strength Factors of Response Corresponding to the First 20 Forcing Modes for Wintertime(10^3)

Order	1	2	3	4	5	6	7	8	9	10
Factor	0.375	0.315	0.237	0.227	0.212	0.200	0.194	0.188	0.179	0.166
Order	11	12	13	14	15	16	17	18	19	20
Factor	0.160	0.153	0.151	0.146	0.143	0.142	0.134	0.129	0.127	0.120

The structure of the first 20 forcing modes is analysed. The efficient forcings have apparently 4 dominant patterns: East Asia–West Pacific pattern, North Africa pattern, West Atlantic pattern and Arctic pattern. Fig. 1 shows the typical structure of the 4 forcing patterns. Each patterns possesses considerably localized structure. It is suitable to name each pattern after the geographical position of the main forcing. So it is suggested that only some of the regions of forcing will result in large responses.

The strength factor of response to the forcings of those 4 patterns has significant variation. The first forcing mode is apparently East Asia / West Pacific pattern, so one can know that the forcings of the East Asia / West Pacific pattern have the largest strength factor of response. This result is consistent with the GCM experiments (see Keshavamurty, 1982; Simmons et al. 1983). The strength factors of response decrease in turn for East Asia / West Pacific pattern, North Africa pattern, West Atlantic pattern and Arctic pattern, and they have the proportion relationship: 3.8 / 2.2 / 1.9 / 1.5. From this proportion relationship, one can find that if anomalous forcings have same strength, the amplitude of the response to the forcing of East Asia / West Pacific pattern is twice as large as that of the response to the forcing

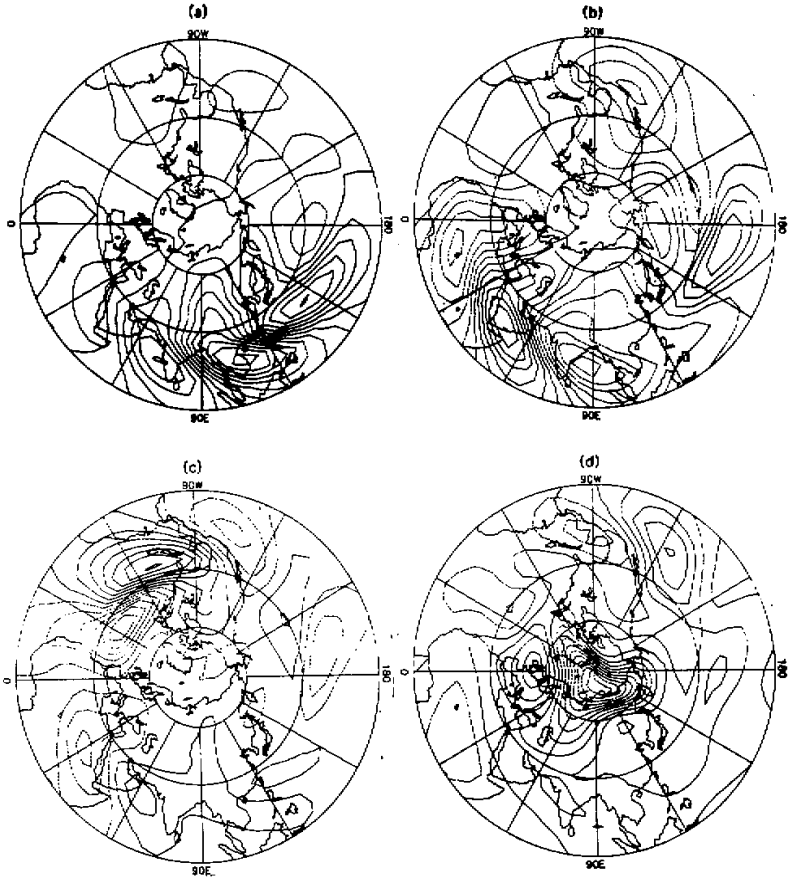

Fig. 1. The typical modes of the 4 efficient forcing patterns for wintertime with the evolution time of 48 hours: East Asia / West Pacific pattern—the 1st forcing mode(a); North Africa pattern—the 3rd forcing mode (b); West Atlantic pattern—the 7th forcing mode (c); Arctic pattern—the 12th forcing mode (d).

of the West Atlantic pattern. So the strength factors of response vary considerably with different locations of forcings.

Some previous numerical studies for example, Keshavamurty (1982) and Simmons (1982) have shown that the response to an anomalous external forcing is greatly influenced by the local structure of the westerly jet. We will show that the locations of efficient forcings highly depend on the local structure of the westerly jet. Fig. 2a shows the 300 hPa climatological wintertime zonal wind. The 3 jet cores can be found on the westerly jet at about 30°N. The jet core with the largest strength is located over the West Pacific. Other two are located over the West Atlantic and North Africa, and they have close strength. Comparing

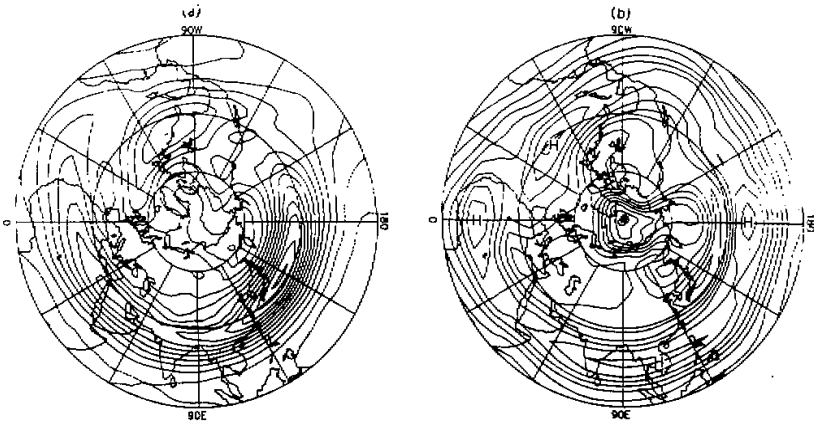

Fig. 2. The 300 hPa climatological winter zonal component of wind (a) and the RMS of the first 20 first forcing modes (b).

Fig. 1 with Fig. 2a, we can find that the main forcings of each pattern are localized to the south of the regions of corresponding jet core, and the strength factor of response matches up well the strength of the jet core. In order to show more clearly the dependence of efficient locations on the local structure of the westerly jet, and verify the dominance of efficient forcings of the 4 forcing patterns, we have computed the root–mean–square (RMS) of the first 20 forcing modes which is displayed in Fig. 2b. The relative large RMS is found to the south of the regions of the westerly jet, and there exist 3 main high centers to the south of the region of the jet core. In addition, there is a maximum of RMS over the polar region. Therefore, the main efficient forcings are localized to the south of the regions of the jet cores, and the strength of the jet core determines the strength factor of response to a great extent.

Except those over the polar region, the efficient forcings have specific spatial structure. They are composed of a chain of highs and lows with southeast to northwest axes. As predicted by the theory of wavepacket (see Lu, 1981; Zeng, 1982), the response to the forcing like this will efficiently extract kinetic energy from the basic flow, and the amplification of a response to an efficient forcing results from the conversion of the kinetic energy of the basic state to the response kinetic energy. Thus, the features of the structure of efficient forcing are related to the instability of the westerly jet.

2. *Summertime*

In section IV—1, we have addressed the efficient forcings for wintertime and pointed out that the features of the efficient forcings are primarily determined by the local structure of the westerly jet. The strength of the summertime westerly jet is considerably weaker than that of the wintertime westerly jet, and there are significant differences in their structure. It can be expected that there are a great deal of differencs in the features of efficient forcing.

Table 2 shows the strength factor of response corresponding to the first 20 forcing modes for evolution time of 48 hours. As expected, the strength factor also decreases rapidly with order index. It is found that the 20th strength factor is only about a second of the first one. The strength factors for summertime are reduced by about a factor of 2 compared with those for wintertime. We have pointed out that the response produced by the efficient forcing will

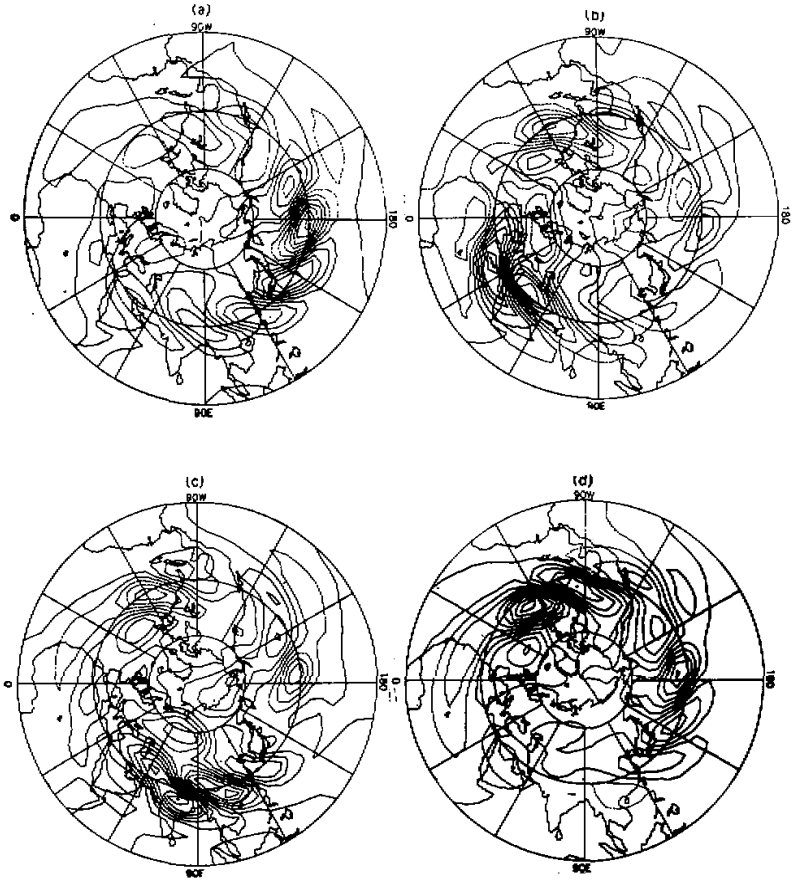

Fig. 3. The typical modes of the 4 efficient forcing patterns for summertime with the evolution time of 48 hours: Middle and West Pacific pattern—the 1st forcing mode (a); East Asia—the 6th forcing mode (b); North Africa pattern—the 4th forcing mode (c); West Atlantic pattern—the 2nd forcing mode (d);

efficiently extract the kinetic energy of the basic state. Because of the weakness of the westerly jet, the response can not gain the kinetic energy of the basic state for summertime as efficient as for wintertime. Therefore, the small strength factor of response for summertime can be explained by the weakness of the westerly jet.

Table 2. Strength Factors of Response Corresponding to the First 20 Forcing Modes for Summertime(10^3)

Order	1	2	3	4	5	6	7	8	9	10
Factor	0.177	0.169	0.166	0.159	0.155	0.154	0.150	0.144	0.140	0.138
Order	11	12	13	14	15	16	17	18	19	20
Factor	0.131	0.129	0.125	0.123	0.121	0.118	0.113	0.110	0.110	0.105

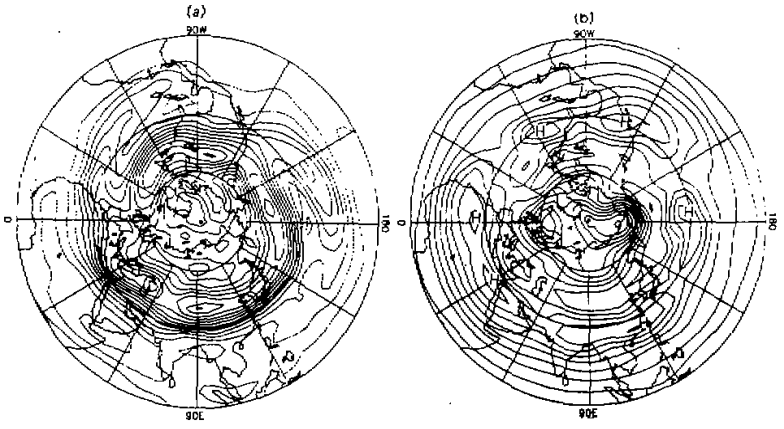

Fig. 4. The 300 hPa climatological summer zonal component of wind (a) and the RMS of the first 20 first forcing modes (b).

The efficient forcings can be grouped into a few patterns like wintertime case. The structure of the first 20 forcing modes is analysed. It is indicated that the efficient forcings have 5 dominant patterns: Middle and West Pacific pattern; North Africa pattern; East Asia pattern; West Atlantic pattern and Arctic pattern. Fig. 3 shows the typical structure of the first 4 patterns. The structure of each pattern is very localized. The strength factors of response vary considerably with different patterns for wintertime case. In contrast, the strength factors are close to each other for different patterns for summertime case, which is due to the nearness of the strength of the jet cores.

The dependence of the features of the efficient forcings on the westerly jet is investigated in the similar manner to the investigation for wintertime case. Fig. 4a shows the 300 hPa summer climatological zonal wind. It can be seen that the main westerly jet is located at about 50°N, where 4 cores are found. The 4 jet cores are centered over the West Pacific, East Asia, North Africa and West Atlantic respectively, and have much the same strength. Comparing Fig. 3 and Fig. 4, one can find that the forcings of the first 4 patterns are localised to the south of the jet cores respectively. We repeat the calculation of RMS of the first 20 forcing modes like wintertime case, which is displayed in Fig. 4b. The large RMS is found to the south of the regions of the westerly jet, and significantly moves northward with the shift of the westerly jet. Furthermore, the regions of the large RMS are characterized by the 4 main high centers, located to the south of the regions of jet cores respectively. It should point out that Arctic region also has large RMS. These results suggest that the efficient forcings are mainly contained in those 5 patterns, and the differences in the features of the efficient forcings result from the differences of the westerly jet between wintertime and summertime cases.

Zeng (1982) has pointed out that the kinetic norm and streamfunction square norm should be used simultaneously in the description of amplification of perturbations. Here, streamfunction square norms are employed and the calculation is repeated. The results are consistent quantitatively with those for the kinetic norm. In addition, the kinetic energy norm is still employed, but the dissipation coefficients are taken as the values which have often been used by, for example, Lau et al. (1992); Hoskins et al. (1993): γ is assigned a value of 1 / (10 days) and K a value of 2.338×10^{16} $m^4 s^{-1}$. The calculation is then repeated, and the conclu-

sions are unchanged quantitatively.

V. CONCLUSION AND DISCUSSION

For linear forcing problems, a method is developed to provide a set of forcing modes which form a complete orthonormal basis for the finite-time response to steady forcing in the energy inner product space. The forcing modes are found by calculating eigenvectors of a positive definite and symmetric matrix determined from given equations of motion. The amplitude of responses to forcing modes is given in terms of the associated eigenvalues. So the leading eigenvectors are naturally the efficient forcings. This method is used in a nondivergent barotropic model linearized about the 300 hPa zonally-varying climatological flow both for northern summertime and wintertime. The results show that the amplitude of response varies considerably with different forcing modes. Only a few of forcing modes associated with the leading eigenvalues can excite significant response.

Some numerical studies have found that the forcing located in the region of West Pacific is most efficient to excite the flow anomalies. Our results support these findings. Moreover, our results indicate other efficient locations, including North Africa region, West Atlantic region, Arctic region, and give the strength factor of the response to the forcing corresponding to these efficient locations. Especially, our results highlight the dependence of the feature of the efficient forcing on the local structure of the westerly jet. The strength and the geographic position of the jet cores to a great extent determine the locations of the efficient forcing and the strength factor of the response. The efficient forcings possess highly localized structure to the south of the regions of the jet cores. In addition, our results show that the efficient forcings are composed of a chain of highs and lows with southeast to northwest axes, and a response produced by an efficient forcing can efficiently extract kinetic energy of the basic state. These findings imply that the amplification of the response is closely related to the instability of the basic state.

Our results suggest that the meridional variations in the basic state can greatly influence the response to external forcing anomalies. The difference in the meridional variations in the basic state will result in the difference in the conversion of the kinetic energy of the basic state to the response kinetic energy. This process naturally acts on teleconnection patterns produced by anomalous external sources. Therefore, the teleconnection patterns should not be determined only by Rossby wave dispersion, and the interaction between the basic state and response can play an important role in the generation of teleconnection patterns.

REFERENCE

Branstator, G. W. (1985), Analysis of general circulation model sea surface temperature anomaly simulations using a linear model, *J. Atmos. Sci.*, **42**: 2225–2254.

Fu Congbin, et al. (1988), Relationship between summer climate in China and the El Nino / Southern Oscillation phenomenon, *Chinese J. Atmos. Sci.* (special issue), 107–116.

Hoskins, B. J., et al. (1981), The steady linear response of a spherical atmosphere to thermal and orographic forcing, *J. Atmos. Sci.*, **38**: 1179–1196.

Hoskins, B.J., et al. (1993), Rossby wave propagation on a realistic longitudinally varying flow, *J. Atmos. Sci.*, **50**: 1661–1676.

Huang Ronghui, et al. (1993), Influence of the heat-source anomaly over the western tropical Pacific on the subtropical high over East Asia during summer and its physical mechanism, in *Frontiers in Atmospheric Sciences*, 132–144, Allerton Press Inc, New York, 1993.

Keshavamurty, R. N. (1982), Response of the atmosphere to sea surface temperature anomalies over the equatorial

Pacific and the telcconnections of the Southern Oscillation, *J. Atmos. Sci.*, **39**: 1241–1254.

Lau K.–M., et al. (1992), Dynamics of teleconnection patterns over summertime, *J. Climate*, **5**: 142–158.

Lu Peisheng, Zeng Qingcun (1981), Evolution of the perturbations in barotropic atmosphere, *Scientia Atmospherica Sinica*, **5**: 1–8 (in Chinese).

Simmons, A. J. (1982), The forcing of stationary wave motion by tropic diabatic heating, *Quart J. Roy. Metcor. Soc* **108**: 503–534.

Simmons, A. J. et al. (1983), Barotropic wave propagation, instability and atmospheric teleconnection patterns, *J. Atmos. Sci.*, **40**: 1263–1392.

Zeng, Qingcun (1982), On the evolution and interaction of disturbances and zonal flow in rotation barotropic atmosphere, *J. Meteor. Soc.*, Japan, **60**: 24–31.